

# Flexible Shape Control for Automatic Resizing of Apparel Products

Yuwei Meng<sup>1,2</sup> Charlie C.L. Wang<sup>2\*</sup> Xiaogang Jin<sup>1</sup>

<sup>1</sup>State Key Lab of CAD&CG, Zhejiang University, China

<sup>2</sup>Department of Mechanical and Automation Engineering, The Chinese University of Hong Kong, China

## Abstract

We provide a flexible shape control technique in this paper for the automatic resizing of apparel products. The automatic resizing function has become an essential part of the 3D garment CAD systems to generate user customized apparel products for individuals with variant body shapes. The human bodies are usually represented by piecewise linear mesh surfaces with consistent connectivity. The shape of apparel products can then be warped from the space around a human body to the space around another body by computing the new positions of points on apparel products. However, one major limitation of this kind of automatic resizing technique is that the apparel products are always distorted along the shape of the human bodies. This is a required deformation for tight clothes but not an expected result for other types of clothes. To solve this problem, we investigate a method to preserve the shape of user defined features on the apparel products. As the apparel products are often represented by discrete surfaces with non-manifold entities, the existing mesh processing approaches that preserve the local shape cannot be applied here. A new algorithm consisting of three steps is developed in this paper. Firstly, the apparel product is warped from the reference human body to the space around the target human body. Secondly, the shape of features is optimized to match their original shape before the warping. Lastly, discrete surfaces of the apparel product are deformed again under an optimization framework to match their original shapes locally while interpolating the shape of features determined in the previous step.

**Keywords:** Shape control, discrete surface, 3D garment resizing, feature preserved, design automation.

## 1 Introduction

Computer-Aided Design (CAD) has become one of the most indispensable elements in modern industry and its usage has started to spread across the apparel industry in recent decades. The business of apparel industry focuses more and more on the user customized product design, where CAD technology speeds up the prod-

uct development procedure and shortens the time taken from designing to fabricating. An essential part of 3D CAD system used for such kind of user customized design automation is how to automatically resize a designed product worn by a model to fit the variant body shapes of individual customers. A conventional way to provide such an ability is the 2D pattern grading techniques that have existed for hundreds of years [1]. However, the grading procedure heavily depends on the specific style of a garment, and there is no automatic or systematic way to modify a given pattern design to fit the variant shapes of bodies. In practice, the grading procedure used in the fashion industry heavily relies on the experience of designers, and therefore cannot be straightforwardly transferred to a computational procedure.

Recently, computer techniques have been used in the apparel industry to automate and ease such resizing (or grading) procedures by directly modifying the 3D shape of garment [2] and then flattening the reshaped surfaces into planar patterns [3, 4, 5]. Such an approach is more intuitive, given that the ultimate goal is to design a 3D garment. However, it is a heavy task for a designer to repeatedly construct the templates of apparel products and encode them to the semantic features of human bodies – such an interactive encoding procedure must be performed for every new style of products. Another simpler garment resizing method was proposed in [6], which is based on firstly building human bodies represented by mesh surfaces with consistent connectivity [7] and then warping the points of products by the corresponding polygons on different human bodies like the method of [8]. A modified warping method based on a continuous function instead of polygons was presented in [9] to improve the shape of resized products. Although such a method works well on the tight garments like T-shirt and jeans pants, unaccepted results with unwanted distortions on the surface regions of garments that are not near the human body are generated. More specifically, the method relies too much on the shape of human bodies which therefore somehow amplifies the defects of the body shape on the resized apparel products (e.g., as the distorted shapes shown in Fig.1).

In this paper, we develop a new method to control the shape of apparel products during the automatic resizing procedure more flexibly. As illustrated in Fig.2, our algorithm consists of three steps. Firstly,

---

\*Corresponding Author; E-mail: cwang@mae.cuhk.edu.hk



Figure 1: Shape control for the 3D automatic resizing of apparel products can be flexibly performed by specifying features (illustrated by the white dashed curves) on the apparel products. The shape of resized products around the features is processed to match the designed shape. This improves the quality of shape on the results of automatic resizing. From left to right, the designed dress worn on a model, side view of the designed dress, the automatic resizing result without shape control on the features using the method of [Wang et al. 2005], our result with the shape of features preserved, the automatic resizing result without shape control, and our result giving straight profiles as the designed shape of the dress.

the apparel product is warped from the reference human body to the space around the target human body (see Fig.2(a)). Secondly, the shape of features is optimized to match their original shape before the warping (shown in Fig.2(b)). Lastly, discrete surfaces of the apparel product are deformed again under an optimization framework to match their original shapes locally while interpolating the shape of features defined in the previous step (see Fig.2(c)). The two-manifold local mesh surface does not always exist in the apparel products, which are often represented by discrete surfaces with polygon soups, hanged edges, and even point sets. Therefore, the existing local shape preserved mesh editing tools [10, 11, 12], which need two-manifold surfaces, cannot be directly applied here. Moreover, for the complex apparel products, the number of vertices on their surfaces may be huge (e.g., more than one million vertices); thus, it is impractical to solve large linear systems with such sizes for the surface processing (as [13, 14]) even if the coefficient matrix is sparse. Our new method can solve such huge linear systems in an efficient way.

The main contribution of this paper falls into two aspects:

- A new shape matching based method to preserve the shape of features defined on apparel products, where the features can be easily specified on apparel products with very simple interactions.
- A new shape optimization method, which can be applied to discrete surfaces containing non-

manifold entities and does not need to solve large linear systems.

These result in a flexible shape control tool for the automatic resizing of apparel products.

The rest of the paper is organized as follows. After reviewing the related work in section 2, we briefly describe the method to warp the shape of apparel products in the spaces around human bodies in section 3. Section 4 details how to preserve the shape of features on the resized garments. The surface optimization method is introduced in section 5 to let the discrete surface of apparel products interpolate the shape of features. The experimental results of our implementation are demonstrated in section 6, and our paper ends with the conclusion section.

## 2 Related Work

The CAD systems used in the apparel industry can be classified into two categories. One follows the traditional garment production procedure that design 2D patterns then try it on in a virtual way by sewing them together to see the virtual fitting result, which is considered as 2D => 3D methods. 2D pattern design systems have been used to help designers simplify their work. The traditional 2D CAD systems provide 2D grading tools to generate patterns of different sizes from the basic pattern set, and then use them to make garments. In fact,

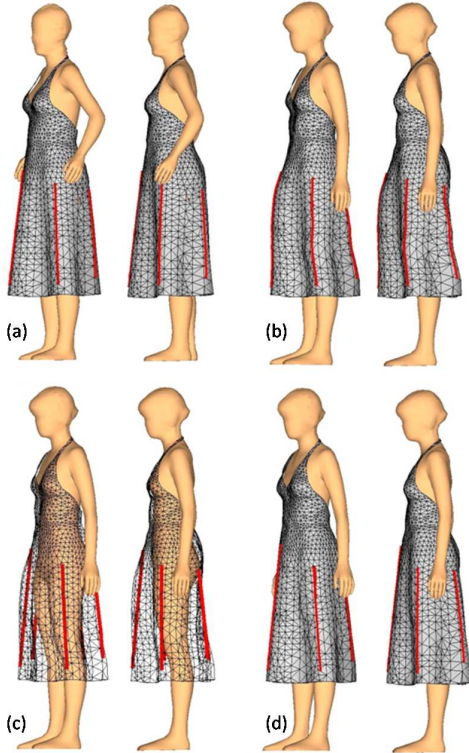


Figure 2: The steps of our flexible shape control algorithm for automatic resizing: (a) the given dress with shape preserving features defined as red lines, (b) the result of primary 3D resizing based on deformation – the shape of features is not preserved, (c) the shape of features is optimized to match its shape before resizing, and (d) the surface shape of the dress is processed to interpolate the shape of optimized feature curves.

it takes years for a person to become an excellent pattern maker. Even a design of simple garments such as T-shirts and skirts calls for the expertise of an experienced pattern maker. Therefore, the industry has recently started to look into 3D features, which take full advantages of computer techniques.

An online made-to-measure system was presented by Cordier et al. [15], in which the system allows virtual try-on of garments on the web according to shoppers’ body measurements. Some simple interactive tools were proposed to edit the garment surface. Parametric curves were used to control the silhouette of garment shape more easily in the work of [16]. The authors of [2, 6] proposed four simple modification tools for the generated garment surface by 2D sketches, which were mesh painting, mesh extrusion, mesh cutting and mesh partition. Then, an automatic resizing technique akin to the t-FFD technique in [8] was employed to make the design product fit with the variant body shapes of individuals. The automatic resizing tools developed in these systems work well on the tight garments but may generate unwanted distortions since the resizing relies too much on the shape of human bodies. Studies show that when

the apparel product is away from the human body, the perfect shape of an apparel product should be locally similar to its shape before resizing. The flexible shape control algorithm presented in this paper is motivated by this observation.

Some non-homogeneous resizing methods have been proposed in the computer graphics area to either modify an image or deform a 3D model. A simple image operator called *seam carving* was presented in [17] to support content-aware image resizing for both reduction and expansion. Kraevoy et al. proposed a method in [18] that protects model features and structures during resizing for complex models, which is considered as a non-homogeneous resizing. Recently, Gal et al. [19] introduced a shape editing method by applying systematic solutions in feature curves extraction, analysis, edit and deformation. However, the method proposed in their paper can only be used in some mechanical objects that have explicitly sharp features. The feature preservation function provided in [19] can hardly be applied to the apparel products which are mainly formed by freeform surfaces. The concept of styling feature curves was also inspired by [16], where they presented some interactive techniques to design 3D garments with parametric contour curves and style curves. However, this paper focuses on a new problem about how to use feature curves to control the shape of apparel products. Although the above techniques can make the resized results feasible, they cannot be employed to realize garment resizing for industrial usage while the techniques presented in this paper can.

### 3 Primary 3D Resizing

This section presents the primary method for 3D resizing, which is similar to the deformation technique presented in [6]. However, to make this paper self-contained, the key steps are briefly introduced here.

Given two human bodies  $H_A$  and  $H_B$  represented by triangular mesh surfaces with consistent connectivity, any triangle  $T \in H_A$  has one and only one corresponding triangle  $T' \in H_B$ , and any vertex  $\mathbf{v} \in H_A$  also has a unique corresponding vertex  $\mathbf{v}' \in H_B$ ; vice versa. Without loss of generality, the apparel product is represented by a non-manifold mesh surface [2] consisting of polygons, edges and even sets of points. Considering model of an apparel product  $M$  designed in the space around the human body  $H_A$ , we are going to define a mapping function  $\Phi(\mathbf{p})$  to obtain a warped shape  $M'$  for the apparel product that  $\forall \mathbf{p} \in M$

$$\mathbf{p}' = \Phi(\mathbf{p}) \quad (\forall \mathbf{p}' \in M'). \quad (1)$$

Here, we adopt an implicitly defined mapping function  $\Phi(\cdot \cdot \cdot)$ . Firstly, the closest point  $\mathbf{q}$  to  $\mathbf{p}$  among all centers  $\mathbf{c}_T$  of the triangles  $T \in H_A$  is searched by using the *Approximate Nearest Neighbor* (ANN) search presented in [20]. The set of triangles that contributes to

the mapping of point  $\mathbf{p}$  is then defined as

$$\Upsilon_{\mathbf{p}} = \{T_i \mid \|\mathbf{p}c_{T_i}\| < (1 + \alpha)\|\mathbf{p}\mathbf{q}\|, \forall T_i \in H_A\} \quad (2)$$

with  $\alpha = 0.2$  in all our tests. Secondly, a local orthonormal frame  $(\hat{\mathbf{u}}_i, \hat{\mathbf{v}}_i, \hat{\mathbf{w}}_i)$  is established at the center  $\mathbf{c}_{T_i}$  of every triangle  $T_i \in \Upsilon_{\mathbf{p}}$ , and a similar frame  $(\hat{\mathbf{u}}'_i, \hat{\mathbf{v}}'_i, \hat{\mathbf{w}}'_i)$  can also be constructed at the corresponding triangle  $T'_i \in H_B$  of  $T_i$ . Thirdly, the local coordinate  $(u_i, v_i, w_i)$  of  $\mathbf{p}$  at the frames  $(\hat{\mathbf{u}}_i, \hat{\mathbf{v}}_i, \hat{\mathbf{w}}_i)$  can be evaluated, which satisfies

$$\mathbf{p} = \mathbf{c}_{T_i} + u_i\hat{\mathbf{u}}_i + v_i\hat{\mathbf{v}}_i + w_i\hat{\mathbf{w}}_i. \quad (3)$$

Lastly, the new position  $\mathbf{p}'$  can be computed by a blending of newly determined positions on these local frames of  $T'_i \in H_B$  as

$$\mathbf{p}' = \frac{\sum_{T_i \in \Upsilon_{\mathbf{p}}} \varpi_i (\mathbf{c}_{T_i} + u_i\hat{\mathbf{u}}'_i + v_i\hat{\mathbf{v}}'_i + w_i\hat{\mathbf{w}}'_i)}{\sum_{T_i \in \Upsilon_{\mathbf{p}}} \varpi_i}, \quad (4)$$

where  $\varpi_i = (10^{-8} + (u_i^2 + v_i^2 + w_i^2)^{\frac{3}{2}})^{-1}$  is the weight coefficient for the position blending. By this method, the resized apparel product for the new human body  $H_B$  can be obtained from a designed 3D model  $M$  around the human body  $H_A$  (see Fig.2(b) for an example).

## 4 Features and Shape Matching

The shape of resized apparel product around individuals using the method presented in the above section may generate unwanted distortions by the shape variation on the human bodies. Although this is acceptable for tight-fit clothes, it is not tolerable for some other styles of clothes. Take the dresses shown in Fig.1 as an example, the white ones are generated by the primary 3D resizing, and unwanted profiles are produced due to the distortion in body shape. In this section, we present the details about how to define features and preserve the shape of features in the problematic regions.

### 4.1 Features

There are many types of features used in the CAD approaches of apparel products [6, 21], which includes feature points (1D), feature curves (2D) and feature patches (3D). Among them, we should select a type of feature that can be used to control the shape of the final apparel product in 3D. Moreover, the features must be easy to be specified interactively. Nowadays, the sketch-based interface has become very popular in many 3D applications [22, 23, 24], where the sketched curves take a very important role. Therefore, we adopt curves as features in our approach to conduct flexible shape control for the automatic resizing of apparel products. In our approach, the feature curves are represented by B-spline curves. There are two types of feature curves in our approach. The first type is the features specified by users to control the shape on the resized apparel products, and the second type is the boundary curves of

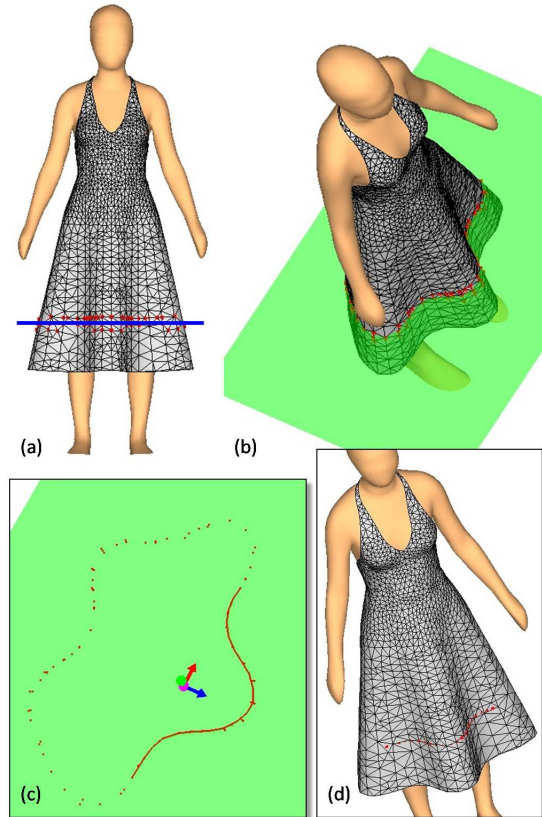


Figure 3: The steps for specifying features on product  $M$ : (a) a line segment specifies the plane to which the feature curve is defined, (b) the plane (in green) to hold the feature curve is rotated and the surface of  $M$  near the plane is projected onto the plane to illustrate a contour of intersection, (c) B-spline curve (in red) is defined on the plane by users, and (d) the B-spline curve is uniformly sampled into a sequence of points (the red ones) attached on the model  $M$ .

the products. However, when the shape of the product is represented by non-manifold entities, the boundary curves may also be specified interactively.

### 4.2 Specifying features on product

As the shape of apparel products could be represented by discrete surfaces with non-manifold entities, the method used to specify feature curves should not rely on the representation of the model  $M$  to be resized. Therefore, every feature curve specified by users is processed as a set of ordered points attached on the 3D model for the apparel product. The steps are described below with the help of an example shown in Fig.3.

First of all, the user can select a viewing direction to draw a line segment (the blue one in Fig.3(a)). When sweeping the line segment along the viewing direction, a plane for specifying feature curves is defined (see the green plane shown in Fig.3(b)) – it is named as *feature plane* in our approach. After that, users can draw B-

Spline curves on the plane to specify the shape as well as range of a feature curve  $\mathbf{c}_f$ . This is because that an apparel product may be represented by polygon soups which cannot always generate a simple curve by intersecting a plane. Many local modification schemes [25] can be used here to control the shape of feature curves to follow the contour of intersection (see Fig.3(c)). Lastly, the feature curve is sampled into a sequence of ordered points  $\bar{\mathbf{c}}_f = \{\mathbf{r}_i\}$  with  $i = 1, \dots, m$ , which is considered as the discrete form of the feature curve  $\mathbf{c}_f$  (see the red points in Fig.3(d)).

All the points sampled from the feature curves are considered as being attached on the apparel product  $M$  and deformed together with  $M$  in the primary 3D resizing step. Then, each sample point  $\mathbf{r}_i$  is mapped to a corresponding point  $\mathbf{r}'_i \in \mathbb{R}^3$  around the new human body  $H_B$  by Eq.(3). The positions of  $\mathbf{r}'_i$ s are optimized so that the feature curves preserve their shapes before resizing.

### 4.3 Shape matching on features

The shape of a deformed feature curve  $\bar{\mathbf{c}}'_f = \{\mathbf{r}'_i\}$  must be optimized in feature plane to match its original shape defined on  $\bar{\mathbf{c}}_f$ . Here the shape of two curves is defined as similar when the relative distributions of the sample points on them are similar to each other. A clearer definition on the similarity is defined below, and the shape of a feature curve will be modified under an optimization framework.

First of all, the new feature plane holding the feature points  $\{\mathbf{r}'_i\}$  must be estimated. Here, the feature plane is computed by the *Principal Component Analysis* (PCA) of all the sampled points (ref. [26]). We randomly generate some auxiliary points  $\{\mathbf{a}_i\}$  near the points  $\{\mathbf{r}_i\}$  on the feature plane before the primary 3D resizing so that the feature plane can be estimated more robustly. The auxiliary points are also mapped to a new position by Eq.(4), and the mapped new points are then added into the PCA for computing the new feature plane.

Assume that every sample point  $\mathbf{r}'_i$  is optimized to a new position  $\mathbf{r}^*_i$ , the local shape similarity at  $\mathbf{r}^*_i$  is measured by its distance to its predicted positions defined by the local frames of the feature curve at  $\mathbf{r}^*_{i+1}$  and  $\mathbf{r}^*_{i-1}$ . Specifically,  $\alpha_i^+$  is computed as the projected length of the vector  $\mathbf{r}_{i+1}\mathbf{r}_i$  on the vector  $\mathbf{r}_{i+1}\mathbf{r}_{i+2}$ , and  $\beta_i^+$  is the projected length of  $\mathbf{r}_{i+1}\mathbf{r}_i$  on  $\mathbf{R}(\mathbf{r}_{i+1}\mathbf{r}_{i+2})$  with  $\mathbf{R}$  being the orthogonal 2D rotation matrix

$$\mathbf{R} = \begin{bmatrix} 0 & 1 \\ -1 & 0 \end{bmatrix}$$

on the feature plane. Therefore, the predicted position of  $\mathbf{r}^*_i$  by the frame at  $\mathbf{r}^*_{i+1}$  is defined as

$$\mathbf{r}_i^+ = \mathbf{r}^*_{i+1} + \alpha_i^+ \mathbf{r}^*_{i+1} \mathbf{r}^*_{i+2} + \beta_i^+ \mathbf{R}(\mathbf{r}^*_{i+1} \mathbf{r}^*_{i+2}). \quad (5)$$

Similarly, another prediction of  $\mathbf{r}^*_i$  is computed by the frame at  $\mathbf{r}^*_{i-1}$  as

$$\mathbf{r}_i^- = \mathbf{r}^*_{i-1} + \alpha_i^- \mathbf{r}^*_{i-1} \mathbf{r}^*_{i-2} + \beta_i^- \mathbf{R}(\mathbf{r}^*_{i-1} \mathbf{r}^*_{i-2}), \quad (6)$$

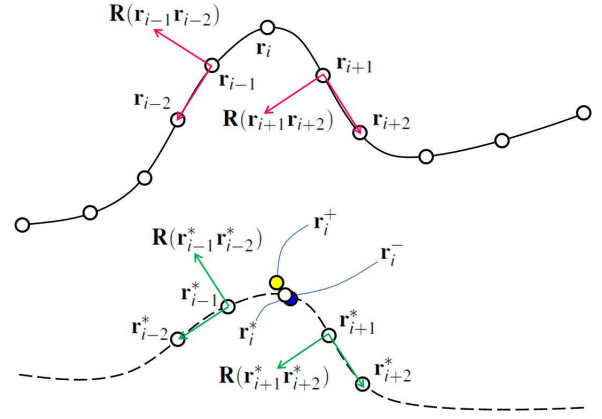


Figure 4: The illustration of modeling local shape similarity by local frames on the sample points: (top) two local frames for computing  $(\alpha_i^-, \beta_i^-)$  and  $(\alpha_i^+, \beta_i^+)$  at  $\mathbf{r}_{i-1}$  and  $\mathbf{r}_{i+1}$  respectively, and (bottom) the differences between the predicted positions  $\mathbf{r}_i^-$  (in blue) and  $\mathbf{r}_i^+$  (in yellow) computed by the new local frames and the optimized position  $\mathbf{r}_i^*$  are minimized during the optimization.

where  $\alpha_i^-$  and  $\beta_i^-$  are the projected lengths of  $\mathbf{r}_i \mathbf{r}_{i-1}$  on  $\mathbf{r}_{i-1} \mathbf{r}_{i-2}$  and  $\mathbf{R}(\mathbf{r}_{i-1} \mathbf{r}_{i-2})$  respectively. An illustration is given in Fig.4.

When  $\mathbf{r}_i^* = \mathbf{r}_i^+ = \mathbf{r}_i^-$ , the local shape at  $\mathbf{r}_i^*$  is defined as *similar* to the local shape at  $\mathbf{r}_i$  of the feature curve  $\bar{\mathbf{c}}_f$  before resizing. The global similarity energy of the optimized feature curve is then defined as

$$E_r = \sum_i \|\mathbf{r}_i^* - \mathbf{r}_i^+\|^2 + \|\mathbf{r}_i^* - \mathbf{r}_i^-\|^2, \quad (7)$$

where a rigid transformation and scaling of the feature curve gives zero energy value. Moreover, we also hope to keep the optimized result close to the shape before optimization. So a deformation energy is defined as

$$E_d = \sum_i \|\mathbf{r}_i^* - \mathbf{r}'_i\|^2 \quad (8)$$

with  $\mathbf{r}'_i$  being the position before optimization. The optimized positions of sample points on the feature plane can finally be computed by solving the following optimization problem

$$\min_{\mathbf{r}_i^*} \varpi_r E_r + \varpi_d E_d, \quad (9)$$

where  $\varpi_r$  and  $\varpi_d$  are the weights to balance these two energy terms during the optimization. As the shape similarity is more of our concern in this approach, we choose  $\varpi_r = 1.0$  and  $\varpi_d = 0.1$ . This is a least-square non-linear optimization problem, which can be easily solved by computing a least-square solution of an over-determined linear equation system derived from the first derivatives of Eq.(9). More details can be found in [27].

When minimizing the global similarity energy  $E_r$ , if no point on the feature curve is fixed, any rigid transformation of the original feature curve  $\bar{\mathbf{c}}_f$  in the new feature

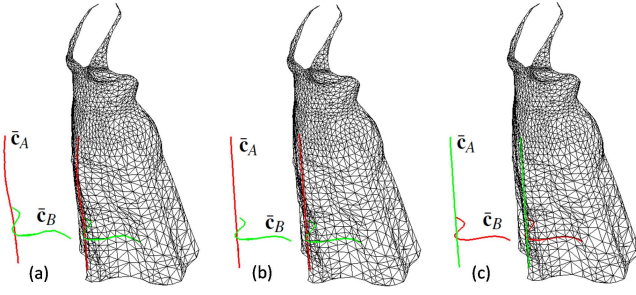


Figure 5: Processing two intersected feature curves,  $\bar{c}_A$  and  $\bar{c}_B$ , in different orders results in feature curves with slightly different shapes: (a) two crossed feature curves on the product before shape optimization, (b)  $\bar{c}_A$  is processed followed by the shape optimization on  $\bar{c}_B$ , and (c)  $\bar{c}_B$  is processed first and then  $\bar{c}_A$ .

plane will lead to the minimum of  $E_r$ . The solution is not uniquely defined. When one sample point (e.g.,  $\mathbf{r}_j$ ) in  $\bar{c}'_f$  is fixed during the optimization, any rotated transformation of  $\bar{c}_f$  around  $\mathbf{r}_j$  also gives a minimal value on  $E_r$ . Therefore, it should have at least two points fixed during the optimization. The selection of two points to be fixed is based on the following heuristics:

- The points which are closer to the human body have higher priority to be fixed since the shape of the apparel product should follow the surface of human body when near it;
- The points close to the feature curves that have already been processed would more likely be fixed as we do not wish the optimization on this feature curve to affect the processed ones.

Therefore, two closest points to the human body with distances  $d_1$  and  $d_2$  are first found as well as other two points nearest to the feature curves that have been processed (with distances  $d_3$  and  $d_4$ ). Among these four points, two points with the smallest value in  $d_k$  ( $k = 1, \dots, 4$ ) are fixed during the optimization.

It should be noted that, when the samples are close to the ends of the feature curve – i.e.,  $\mathbf{r}_i$  with  $i < 3$  or  $i > m - 3$ , the formulas in Eqs.(5) and (6) may be invalid. Those invalid formulas are discarded from the least-square linear system for minimizing the objective function in Eq.(9). When a feature curve is closed, the indices in Eqs.(5) and (6) are recycled to make the formulas valid.

The feature curves defined by users sometimes intersect with each other (e.g., the two curves shown in Fig.5). To make the optimizations conducted on two feature curves  $\bar{c}_A$  and  $\bar{c}_B$  compatible, the intersection point  $\mathbf{p}_{int}$  should be explicitly defined. Firstly, the shape of  $\bar{c}_A$  is processed according to what we have proposed above. Then, when processing  $\bar{c}_B$ , the intersection point  $\mathbf{p}_{int}$  on it is fixed by its position determined during the shape optimization of  $\bar{c}_A$ . The order to process the shape of feature curves follows the order of how

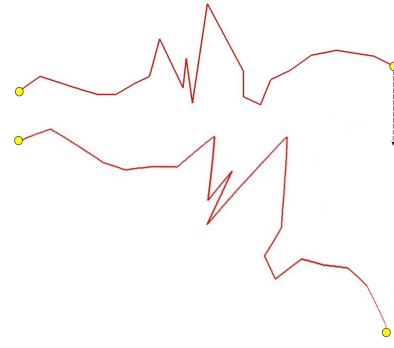


Figure 6: The proposed shape matching method for deforming feature curves can well preserve the local shapes. When dragging one endpoint of a curve while fixing the other one (top), the resultant curve (bottom) can still present the original zig-zag shape very well.

user specifies them based on a heuristic that a more important feature curve are specified earlier. As illustrated in Fig.5, processing the intersected feature curves in different orders results in feature curves with different shapes.

The above proposed shape matching method works fine on preserving the local shape of feature curves. See Fig.6 for an example, where the shape angles of the zig-zag shape on the given feature curve are well-preserved on the deformed feature curve. However, this method cannot preserve the higher order or global features such as circularity, orthogonality, parallel, etc.

## 5 Shape Optimization of Discrete Surface

This section presents the details about how to update the shape of the discrete surface for an apparel product. The updated discrete surface should interpolate the optimized feature curves computed by the method proposed above and meanwhile preserving the local shape presented on the discrete surface.

### 5.1 Sampling and construction of local support

As the discrete surface for an apparel product may be represented by polygon soups which in general do not provide a correct local support, we sample the surface warped from  $M$  into a set of points  $\bar{M}$  to make our algorithm general and robust. However, this may result in too many samples. To speed up the computation, we downsample the points of  $\bar{M}$  into fewer points by

- partitioning the bounding box of  $\bar{M}$  uniformly into voxels,
- and then using the sample point of  $\bar{M}$  in a voxel, which is nearest to the center of the voxel, as an agent of the discrete surface  $\bar{M}$ .

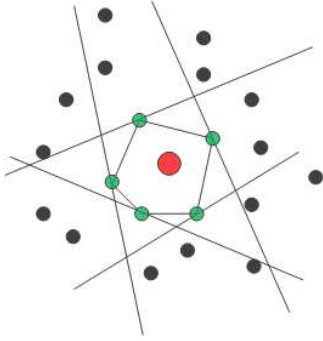


Figure 7: Searching for the one-ring neighbors (in green) of a given agent point  $\mathbf{a}$  (in red color).

The sampled points on feature curves are also considered as agents of  $\bar{M}$ . The shape optimization of the discrete surface is conducted on these agents.

For every agent point  $\mathbf{a}$ , the local support is established by determining its one-ring neighbors. The method of [28] is employed here, the efficient implementation of which needs the help of a fast closest point query as [20].

1. The nearest agent point  $\mathbf{a}_c$  to  $\mathbf{a}$  is searched and considered as one of its one-ring neighbors;
2. All the agent points  $\mathbf{p}$  *above* or *on* the plane  $(\mathbf{p} - \mathbf{a}_c) \cdot (\mathbf{a}_c - \mathbf{a}) = 0$  are excluded from the further neighborhood search;
3. Repeating step 1 and 2 until no point exists in the search.

As illustrated in Fig.7, the planes determined in this search algorithm actually define a convex hull around the agent point  $\mathbf{a}$ , which contains only this agent point (i.e., no other agent point is inside the convex hull). All the agent points lying on the convex hull are considered as the one-ring neighbors of  $\mathbf{a}$ .

## 5.2 Local shape encoding

The purpose of shape optimization of the discrete surface  $\bar{M}$  is to deform it to a shape interpolating the feature curves (i.e., the agents defined by the sample points on feature curves). During the deformation, we wish to maintain the local shape and the geometric details on  $\bar{M}$ . Therefore, a method to encode the relative spatial relationship between an agent point  $\mathbf{a}$  and its one-ring neighbors is needed. Since this relationship is employed in the shape optimization of  $\bar{M}$ , it should have the following properties.

- The relationship between the positions of  $\mathbf{a}$  and its one-ring neighbors  $\mathbf{a}_i$  ( $i = 1, \dots, k$ ) must be a linear combination so that the shape optimization can be solved efficiently.
- The encoding of relationship considers the non-uniformity of the distribution of  $\mathbf{a}_i$  around  $\mathbf{a}$ .

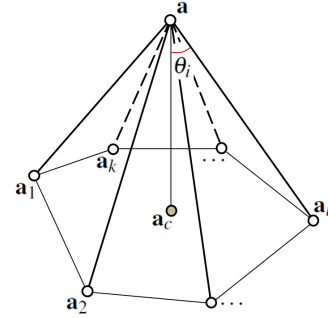


Figure 8: Local shape encoding for the agents around  $\mathbf{a}$ , where  $\mathbf{a}_c$  is the weighted average of its one-ring neighbors as defined in Eq.(11).

- As the number of agents may be very large, we plan to encode the relationship into a weakly diagonal dominated linear equation system – therefore the convergency of using Gauss-Seidal method<sup>1</sup> [29] to solve the linear system is guaranteed.

A new local coordinate encoding method is investigated below to satisfy all these requirements.

As illustrated in Fig.8, we first compute the weighted average point of  $\mathbf{a}$ 's one-ring neighbors,  $\mathbf{a}_i$ . Here, we adopt a weighting method according to the inverse square distance between  $\mathbf{a}_i$  and  $\mathbf{a}$  as

$$\lambda_i = \frac{\|\mathbf{a}_i\mathbf{a}\|^{-2}}{\sum_{j=1}^k (\|\mathbf{a}_j\mathbf{a}\|^{-2})}, \quad (10)$$

which satisfies  $\sum_{i=1}^k \lambda_i \equiv 1$ . The weighted average

$$\mathbf{a}_c = \sum_{i=1}^k \lambda_i \mathbf{a}_i \quad (11)$$

can then be obtained. The angle  $\theta_i$  between the vectors  $\mathbf{a}\mathbf{a}_c$  and  $\mathbf{a}\mathbf{a}_i$  is computed for encoding the relationship between  $\mathbf{a}$  and  $\mathbf{a}_i$  in the local pyramid. Finally, the local coordinate is encoded as

$$\mathbf{a} = \sum_{i=1}^k \lambda_i \mathbf{a}_i + \sum_{i=1}^k \lambda_i (\mathbf{a} - \mathbf{a}_i) \cos \theta_i + \mathbf{h} \quad (12)$$

with  $\mathbf{h}$  being a compensation vector. This satisfies the convergency condition of using Gauss-Seidal method to compute the optimized positions of agent points – the linear equation system is weakly diagonal dominated. Analysis will be given in the following subsection.

## 5.3 Controlled reconstruction

The positions of all agent points are firstly updated, and all vertices on the warped model of the given apparel

<sup>1</sup>When using Gauss-Seidal method to solve a linear equation system, the solution can be obtained by updating the variables in the out-of-core manner; therefore, a very huge linear equation system can still be processed easily.

product are moved to the blended positions by the local frames defined on the agent points thereafter.

The agent point  $\mathbf{a}_j$  not belonging to any feature curve and far away from the human body (e.g., more than  $\epsilon = 1\text{cm}$  in the application of apparel product) is updated to a new position  $\mathbf{a}_j^*$ . The new positions of agent points should retain a local relationship as defined in Eq.(12) as

$$\mathbf{a}_j^* = \sum_{i=1}^k \lambda_i \mathbf{a}_i^* + \sum_{i=1}^k \lambda_i (\mathbf{a}_j^* - \mathbf{a}_i^*) \cos \theta_i + \mathbf{h}_j. \quad (13)$$

When the distance between  $\mathbf{a}_j$  and the human body is less than  $\epsilon$ , we must fix its position by

$$\mathbf{a}_j^* = \mathbf{a}_j. \quad (14)$$

When the agent point  $\mathbf{a}_j$  belongs to a feature curve, its position must be updated by

$$\mathbf{a}_j^* = \mathbf{r}_j^* \quad (15)$$

with  $\mathbf{r}_j^*$  being its optimized position on the feature curve (by the method presented in section 4). In this linear equation system, Eq.13 can be updated into

$$(\sum_{i=1}^k \lambda_i (1 - \cos \theta_i)) \mathbf{a}_j^* - \sum_{i=1}^k \mathbf{a}_i^* \lambda_i (1 - \cos \theta_i) = \mathbf{h}_j,$$

which satisfies

$$|\sum_{i=1}^k \lambda_i (1 - \cos \theta_i)| = \sum_{i=1}^k |\lambda_i (1 - \cos \theta_i)|$$

by the coefficients of  $\mathbf{a}_j^*$  and  $\mathbf{a}_i^*$  since  $\lambda_i > 0$  and  $1 - \cos \theta_i \geq 0$ . As long as there is one equation like Eq.(14) and/or Eq.(15) in the system, it is a weakly diagonal dominated linear equation system (ref.[29]) and can be solved by the Gauss-Seidal method. Specifically, the initial value of an agent not on the feature curves is assigned as  $\mathbf{a}_j$ . Then, the optimized positions of all such agents are computed by iteratively updating their values according to Eq.(13). When the  $L^2$ -norm of the update vector on all such agents is less than  $10^{-5}$  or the iteration has run more than 500 times, the iteration is terminated.

To update the vertices on the warped model  $M'$  to their optimal positions, we first need to establish local frames on every agent point at their positions before and after the shape optimization. The normals of the triangles defined by  $\mathbf{a}$  and its one-ring neighbors are computed, and their average normal is considered as the surface normal at  $\mathbf{a}$ . The orientation of normals on all agent points is corrected by using the minimal spanning tree based propagation as [26]. The normal vector at  $\mathbf{a}$  is used to define a tangent plane. The local frame at  $\mathbf{a}$  is established by the projection of vector  $\mathbf{aa}_1$  on the tangent plane, the normal vector and their cross-product. Then, for any vertex  $\mathbf{p} \in M'$ , its new position can be determined by

1. computing its local coordinates in the frames at agents whose distance to  $\mathbf{p}$  is less than three times of the width of voxels used in the sampling step;

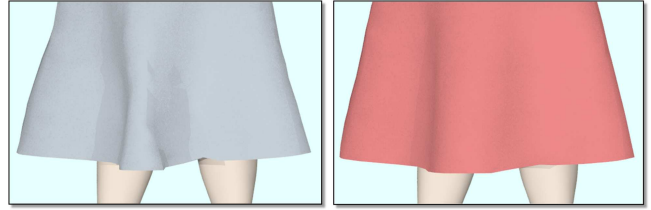


Figure 9: The effect of crossed feature curves shown in Fig.5: (left) the result of primary 3D resizing with unwanted distortion on wrinkles and (right) the result after the shape optimization of the feature curves and the discrete surface.

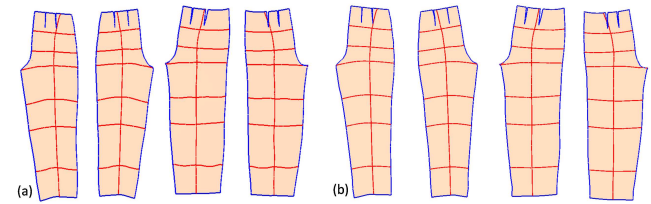
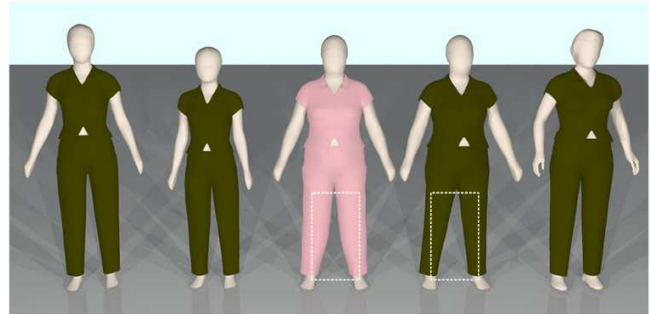


Figure 10: The shape control on a suit. The middle one (in pink) is generated by the deformation based 3D resizing method; from the one at the right of it, it is clear that the profile of pants has been straightened by our approach. (a) and (b) are the 2D patterns of the pants generated by the ARAP surface flattening technique, where (a) is flattened from the pants before applying our shape control approach and (b) is generated from the optimized pants.

2. applying these local coordinates to obtain new positions by the frames on the optimized agent points;
3. blending the positions defined by different frames into a unique position in the manner as shown in Eq.(4).

By this, an optimized shape  $M^*$  for the apparel product can be obtained.

## 6 Results

We have implemented the algorithm presented in this paper in a prototype system using Visual C++. Several examples have been tested on the system.

The first example is the automatic resizing of dresses shown in Fig.1. Without applying the method proposed



in this paper, unwanted distortions are generated on the profiles of dresses resized by the method of [6] (see the white one in Fig.1). After specifying the feature curves at the places where the shape control must be conducted, the shape of resized model on the profiles is well optimized. Fig.9 shows the effect of crossed feature curves specified in Fig.5. The second example shown here is to apply the technique presented in this paper to a suit (see Fig.10), where the 2D patterns are generated from the 3D shape of pants by the *As-Rigid-As-Possible* (ARAP) surface flattening technique presented in [30]. The flattening results on the optimized shape have fewer ‘S’-shape distortions on the red curves, which are semantic feature curves for the apparel industry.

The following three examples are all tested on the apparel products which are represented by non-manifold surfaces. From the results shown in Figs.11-13, we can find that our approach is general and can be successfully applied to the apparel products represented by discrete surfaces. They also demonstrate that the proposed flexible shape control algorithm in this paper can easily be used to improve the shape of the resized 3D models around human bodies.

## 7 Conclusion

In this paper, we present a novel approach for the flexible shape control of automatic resizing for apparel products. In our approach, the shape control is decomposed into two phases. First, shape optimization is conducted on the user specified feature curves in order to preserve their shape on the model before 3D resizing. Second, the shape of discrete surface for the apparel product is deformed to interpolate the optimized shape of feature curves while trying to preserve its original shape locally. A novel local geometry encoding method is introduced to result in a weakly diagonal dominated linear equation system. The solution can then be found in a very efficient way using the Gauss-Seidal method. Several examples have been shown in the result section to demonstrate the functionality of our approach, which provides a very useful tool for the design automation of user customized apparel products.

## Acknowledgments

The research presented in this paper was partially supported by the Hong Kong Research Grants Council (RGC) General Research Fund (GRF): CUHK/417508 and CUHK/417109. Xiaogang Jin was supported by the National Key Basic Research Foundation of China (Grant No. 2009CB320801) and the NSFC-MSRA Joint Funding (Grant no.60970159).

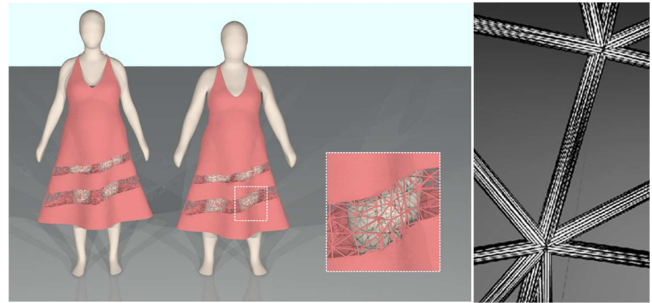


Figure 11: The result of applying our method on a dress model containing complicated non-manifold entities. The zoom-view shows the detailed meshes of the model at the place of non-manifold entities.

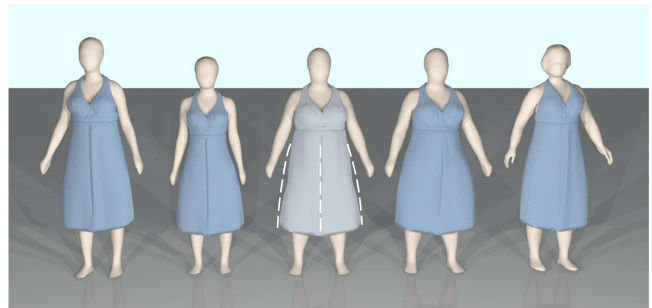


Figure 12: The examples showing the differences between the 3D resizing results obtained with (in blue color) vs. without (in white) applying the shape optimization presented in this paper. The dashed curves show the shape of profiles to be preserved.

## References

- [1] P. J. Taylor, M. M. Shoben, Pattern grading for the Fashion Industry, Cheltenham: Stanley Thornes, 1990.
- [2] C. C. L. Wang, Y. Wang, M. M. F. Yuen, Feature based 3d garment design through 2d sketches, *Computer-Aided Design* 35 (7) (2003) 659–672.
- [3] C. C. L. Wang, S. S. F. Smith, M. M. F. Yuen, Surface flattening based on energy model, *Computer-Aided Design* 34 (11) (2002) 823–833.
- [4] C. C. L. Wang, K. Tang, B. M. L. Yeung, Freeform surface flattening based on fitting a woven mesh model, *Computer-Aided Design* 37 (8) (2005) 799–814.
- [5] C. C. L. Wang, Wirewarping: A fast surface flattening approach with length-preserved feature curves, *Computer-Aided Design* 40 (3) (2008) 381–395.
- [6] C. C. L. Wang, Y. Wang, M. M. F. Yuen, Design automation for customized apparel products, *Computer-Aided Design* 37 (7) (2005) 675–691.
- [7] C. C. L. Wang, Parameterization and parametric design of mannequins, *Computer-Aided Design* 37 (1) (2005) 83–98.
- [8] K. G. Kobayashi, K. Ootsubo, t-FFD: free-form deformation by using triangular mesh, in: *SM '03: Proceedings of the eighth ACM symposium on Solid modeling*



Figure 13: The example of a dress with multiple layers. The profile of the dress is bent (the white one) when only applying the primary 3D resizing. After applying the shape control technique presented in this paper, the shape of the profile is well reconstructed on the resizing result.

- and applications, ACM, New York, NY, USA, 2003, pp. 226–234.
- [9] C. C. L. Wang, K.-C. Hui, K. M. Tong, Volume parameterization for design automation of customized free-form products, *IEEE Transactions on Automation Science and Engineering* 4 (1) (2007) 11–21.
- [10] Y. Lipman, O. Sorkine, D. Levin, D. Cohen-Or, Linear rotation-invariant coordinates for meshes, *ACM Trans. Graph.* 24 (3) (2005) 479–487.
- [11] Y. Lipman, D. Cohen-Or, R. Gal, D. Levin, Volume and shape preservation via moving frame manipulation, *ACM Trans. Graph.* 26 (1) (2007) 5.
- [12] R. W. Sumner, J. Schmid, M. Pauly, Embedded deformation for shape manipulation, *ACM Trans. Graph.* 26 (3) (2007) 80.
- [13] Y. Yu, K. Zhou, D. Xu, X. Shi, H. Bao, B. Guo, H.-Y. Shum, Mesh editing with poisson-based gradient field manipulation, in: *SIGGRAPH '04: ACM SIGGRAPH 2004 Papers*, ACM, New York, NY, USA, 2004, pp. 644–651.
- [14] M. Botsch, M. Pauly, M. Gross, L. Kobbelt, Primo: coupled prisms for intuitive surface modeling, in: *SGP '06: Proceedings of the fourth Eurographics symposium on Geometry processing*, Eurographics Association, Aire-la-Ville, Switzerland, Switzerland, 2006, pp. 11–20.
- [15] F. Cordier, H. Seo, N. Magnenat-Thalmann, Made-to-measure technologies for an online clothing store, *IEEE Comput. Graph. Appl.* 23 (1) (2003) 38–48.
- [16] J. Wang, G. Lu, W. Li, L. Chen, Y. Sakaguti, Interactive 3d garment design with constrained contour curves and style curves, *Computer-Aided Design* 41 (9) (2009) 614–625.
- [17] S. Avidan, A. Shamir, Seam carving for content-aware image resizing, in: *SIGGRAPH '07: ACM SIGGRAPH 2007 papers*, ACM, New York, NY, USA, 2007, p. 10.
- [18] V. Kraevoy, A. Sheffer, A. Shamir, D. Cohen-Or, Non-homogeneous resizing of complex models, in: *SIGGRAPH Asia '08: ACM SIGGRAPH Asia 2008 papers*, ACM, New York, NY, USA, 2008, pp. 1–9.
- [19] R. Gal, O. Sorkine, N. J. Mitra, D. Cohen-Or, iwires: an analyze-and-edit approach to shape manipulation, *ACM Trans. Graph.* 28 (3) (2009) 1–10.
- [20] D. Mount, S. Arya, ANN: A Library for Approximate Nearest Neighbor Searching, <http://www.cs.umd.edu/~mount/ANN/>, 2006.
- [21] C. Au, M. Yuen, Feature-based reverse engineering of mannequin for garment design, *Computer-Aided Design* 31 (12) (1999) 625–634.
- [22] L. Olsen, F. F. Samavati, M. C. Sousa, J. A. Jorge, Sketch-based modeling: A survey, *Computers & Graphics* 33 (1) (2009) 85–103.
- [23] A. Nealen, T. Igarashi, O. Sorkine, M. Alexa, Fiber-mesh: designing freeform surfaces with 3d curves, *ACM Trans. Graph.* 26 (3) (2007) 41.
- [24] E. Turquin, J. Wither, L. Boissieux, M.-P. Cani, J. Hughes, A sketch-based interface for clothing virtual characters, *IEEE Comput. Graph. Appl.* 27 (1) (2007) 72–81.
- [25] L. Piegl, W. Tiller, *The NURBS Book*, Springer, 1997.
- [26] H. Hoppe, T. DeRose, T. Duchamp, J. McDonald, W. Stuetzle, Surface reconstruction from unorganized points, in: *SIGGRAPH '92: Proceedings of the 19th annual conference on Computer graphics and interactive techniques*, ACM, New York, NY, USA, 1992, pp. 71–78.
- [27] K. Madsen, H. Nielsen, O. Tingleff, *Methods for non-linear least squares problems*, Lecture Notes (2004).
- [28] G. Guennebaud, L. Barthe, M. Paulin, Interpolatory refinement for real-time processing of point-based geometry, *Computer Graphics Forum* 24 (3) (2005) 657–666.
- [29] W. Press, S. Teukolsky, W. Vetterling, B. Flannery, *Numerical recipes in C++: the art of scientific computing*, Cambridge University Press, 1992.
- [30] L. Liu, L. Zhang, Y. Xu, C. Gotsman, S. J. Gortler, A local/global approach to mesh parameterization, *Computer Graphic Forum* 27 (5) (2008) 1495–1504.